DESIGN OF INFLATABLE LUNAR STRUCTURE

By

DHEERAJ KUMAR KAJA

A thesis submitted to the

Graduate School-New Brunswick

Rutgers, The State University of New Jersey

in partial fulfillment of the requirements

for the degree of

Master of Science

Graduate Program in Mechanical and Aerospace Engineering

written under the direction of

Professor Haym Benaroya

And approved by

_____

_____

_____

New Brunswick, New Jersey

October 2017

ABSTRACT OF THESIS

DESIGN OF INFLATABLE LUNAR STRUCTURE

By DHEERAJ KUMAR KAJA

Thesis Director:

Haym Benaroya

NASA and other space agencies are now looking to create a lunar settlement for the continued exploration of Moon and beyond. The most challenging aspect of a lunar settlement is its construction, and the weight and size of building materials brought from Earth. In-Situ Resource Utilization (ISRU) and inflatable structures are considered to be the most preferred way for the fabrication of a lunar settlement because they minimize weight and size.

The use and performance of inflatables and flexible structures in space applications have been increased in the recent past due to the technological advancements in materials technology. So, we propose the concept of two-tier semi-rigid inflatable structure where the base is built with the help of autonomous robots using ISRU, and the main inflatable structure is manufactured on Earth and inflated on the lunar surface. Also, magnesium is proposed as the base material as it is the most abundantly available structural-strength material in lunar environment, and it is relatively easy to machine. A hemispherical

inflatable structure placed on top of a cylindrical base with regolith shielding around the structure is considered as a possible lunar design as well as the test prototype.

A static analysis is first conducted on the proposed design using ANSYS, and the stress values are order-of-magnitude verified with simple calculations that prove the possibility of the material and model. Also, an order-of-magnitude analysis is conducted on meteoroid impact loads where we estimate the maximum size of meteoroid that our structure can sustain.

As future work, we suggest the framework known as Performance Based Engineering. We had spent some time attempting to use this framework for a simplified lunar structural analysis. However, large data gaps precluded significant progress. But we include it as one of our future research topics.

Acknowledgements

First and foremost, I wish to express my gratitude to my research advisor Professor Haym Benaroya, who graciously allowed me to build this thesis on his ideas and has guided me throughout this project. I am thankful for his friendship, support, and kindness.

I would like to thank my committee members Professor Haim Baruh and Professor Aaron Mazzeo.

Our Department of Mechanical and Aerospace Engineering has been an enjoyable place to work, and therefore I am thankful to all our faculty members, staff, and my fellow graduate students.

Words cannot express my gratitude to my family. I am truly grateful to my parents, Balarama Krishna Kaja and Leela Kaja, for all their support and love. I should also thank my sister Vanitha Marpadge and her husband Srinivas Marpadge for their continuous support and encouragement.

I have been blessed with many great friends to all of whom I am thankful, especially Prashanth Turla, Lalith Kotamarthy, and Siddharth Krishna.

Last but not least, I wish to thank all the researchers and authors whose work I have used in this thesis

Table of Contents

List of Tables

List of Figures

Chapter 1. Introduction

In aerospace applications, inflatable composite structures are being considered as they offer substantial benefits over orthodox rigid structures. Inflatable structures are flexible, low mass, and can have more complex-shaped volumes than rigid structures, which drastically reduces the launch costs since smaller launch vehicles are needed. Inflatable composite structures are typically manufactured from materials that have higher strength to weight ratios than conventional systems, and are therefore lower in mass.

NASA, in collaboration with Bigelow Aerospace, is currently exploring inflatable composite structures for use as habitats. Space suits, which are comprised of flexible composite components, are a good example of the successful use of inflatable composite structures in space. Space suits work on inflatable technologies to provide a standalone spacecraft for astronauts during extra-vehicular activity. An anticipated extension of this application of inflatable technology is to space and lunar habitat structures.

This is a good time to explore inflatable, and hybrid-inflatable habitat concepts. Good dimensional precision has been obtained in ground test systems and what remains is to prove that such systems have acceptable long-term strength and survivability in the space and lunar environments. Recent developments in inflatables research and manufacturing techniques are helping significantly towards this. Advanced flexible polymers and high-strength fibers such as Kevlar, Vectran, and Spectra have allowed the fabrication of very low mass structures that are deployable from a closely packed state.

Human presence on the Moon could also ease the cost of further exploration, since lunar-based spacecraft could escape the Moon’s lower gravity using less energy at less cost than Earth-based vehicles. The knowledge and data gained on the Moon will

serve as groundwork for human missions beyond the Moon. The ongoing research for a base on the Moon is mostly for energy, science, and commerce, but potentially also for a larger-scale human presence. The comprehensive human existence on the Moon will assist astronauts to develop new technologies and harness the Moon's abundant resources. The Indian Space Research Organization, ISRO, is already planning a mission that will extract helium 3 from the Moon, a substance that can be used as an energy resource by 2030 for potential nuclear fusion reactors [1].

In the thesis we will provide a brief history of inflatables, ongoing research, and future developments for a lunar base.

Chapter 2. LITERATURE REVIEW

2.1 Overview

This chapter summarizes the previous research work on inflatables and rigidized inflatables, current research on inflatables, and the limitations of the existing research.

2.2 History of Inflatables and Rigidized Inflatables

At the beginning of interplanetary explorations, inflatables were tough contenders for heavy structures alongside conventional pre-constructed structures. Inflatables were deployed regardless of the lack in technology, as they were the only alternative to those heavy metallic structures. Table 2.1 shows a list of inflatables flown during early 60's.

SYSTEM	WT (lbs.)	DIA (ft.)	LAUNCH DATE	LIFE (Yrs.)	PURPOSE	FILM THICKNESS
ECHO I	135	100	AUG 1960	5	COMM.	0.5 FILM/VDA
EXPLORER IX	34	12	FEB 1961	3	HI-ALT DENSITY	0.5 FILM (2) 0.5 AL (2)
EXPLORER XIX	34	12	DEC 1963	2	HI-ALT DENSITY	0.5 FILM (2) 0.5 AL (2)
ECHO II	580	135	JAN 1964	-	COMM.	0.35 FILM 0.18 AL (2)
PAGEOS I	149	100	JUN 1966	5	EARTH SURVEY	0.5 FILM VDA (2000)

Table 2. 1. NASA inflated thin film satellites [2]

The Echo I Balloon was propelled into orbit on August 12, 1960, and was designed to be able to regulate radar systems. Inflatable structures could be utilized for space applications as was illustrated by The Echo I Balloon. The Echo I Balloon was intended

to be a seamless sphere that allowed scientists to use analytical equations and to accurately calibrate their radar systems.

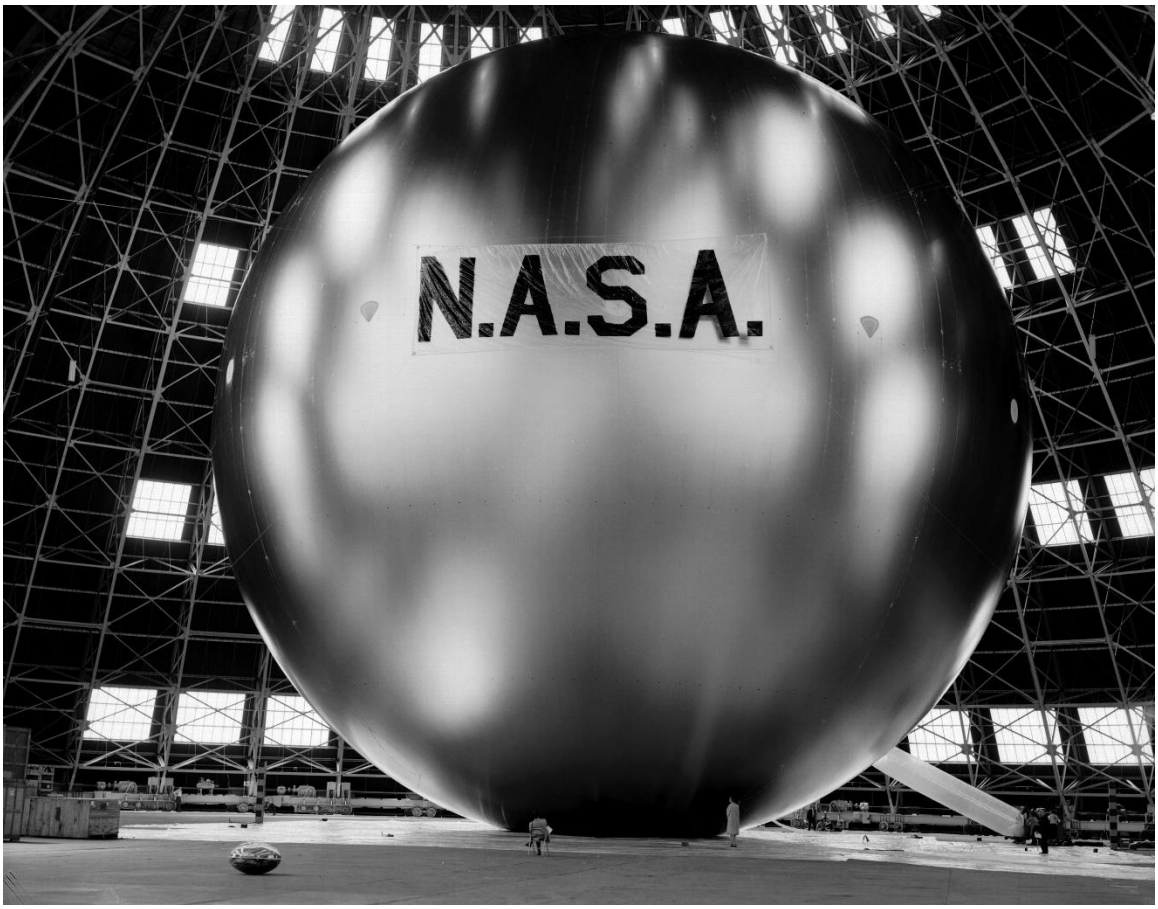

Figure 2. 1. Echo I Balloon (Image courtesy of NASA)

Project Echo I balloon satellite program emphasized the abilities of inflatable structures. The benefits of using inflatable structures can be seen with the Echo I Balloon in regards to its packing efficiency. It had a diameter of 100 feet when fully inflated and could be compressed into a spherical ampule with a diameter of 26 inches. Because of their small, stowed volume, inflatable structures became viable when storage space in lift vehicles became an issue. There is a drastic reduction in weight with the balloon only weighing

136 lb. The Echo I balloon used gases to inflate the internal structure in order to hold the shape of balloon, as an alternative to the traditional internal structures.

In space, rapid leakage of gases from the sphere is a concern, especially when considering meteoroid impact. To resolve the issue, scientists came up with the idea of inflating the material (aluminum) to a point where it yielded a small amount, strain hardened, and became rigid so that the balloon didn't depend only on the gases to maintain its shape [3].

2.3 Materials

Lunar structures should be easily constructed since astronauts cannot be construction workers on the Moon, due to the radiation and thermal environment. One of the important choices we make in modeling lunar structures is to decide on the materials, and this can be difficult since we are unsure of many environmental factors on Moon. One environmental condition that we know quite exactly is that gravity is $1/6^{th}$ that of Earth, i.e., the weight-bearing capacity of an identical structure on the Moon is 6 times that for the Earth. To provide a comfort zone for astronauts, internal pressurization is maintained at 5 psi – 14.7 psi.

Radiation on the Moon is a major factor in designing and selecting the material for the habitat structure. The lunar structure should be shielded from solar, cosmic, electromagnetic radiation, meteoroid impacts, and variations in temperatures that range from 100 to -150 ^{o}C. The lunar surface also has a layer of fine dust that is highly abrasive, which makes it difficult to maintain internal pressure.

In order to overcome the above difficulties, the lunar structure has different layers that shield it from radiation, micrometeoroids, temperature fluctuations, and maintenance of shape. The structural material should have high strength, ductility, durability, puncture resistance, and low coefficient of thermal expansion. Metals like steel and iron can't be used as we can't cast them directly by heating, forging, or extrusion. The infrastructure for casting or forging will not be created early in the lunar settlement process. Metals like titanium have good strength-to-weight ratio but its susceptibility to oxygen, hydrogen and nitrogen makes titanium more brittle. Aluminum and magnesium can be used because they are relatively lightweight, can be cast easily and have good machinability properties. Fabrics are strong contenders for materials as they are manufactured using fibers and then coated for added protection. Among all the fibers, Kevlar is ideal for use in lunar structures because of its high strength-to-weight ratio and tear resistance. Also, it can be coated with other materials for added protection.

Lunar soil or lunar regolith is the most common material available on the Moon. Figure 2.2 shows the composition of the lunar regolith. Table 2.2 shows the average composition of major materials on the lunar surface. Relative density of regolith can be adjusted depending on the compactness of the soil particles, which is an added advantage. Relative densities of soil particles are given in Table 2.3. Regolith is generally used for shielding structures from direct radiation, meteoroid impacts, and temperature variations. A minimum of 2.5 m of regolith cover is required to minimize the radiation levels.

Element	O	Si	Mg	Fe	Ca	Al	Cr	Ti	Mn	H
Amount (wt%)	43.4	20.3	19.3	10.6	3.22	3.17	0.42	0.18	0.12	(a)

Table 2. 2. Average Composition of Major Materials on Lunar Surface [4]

Relative density	Description
0–15	Very loose
15–35	Loose
35–65	Medium
65–85	Dense
85–100	Very dense

Table 2. 3. Conventional Terms of Relative Density [5]

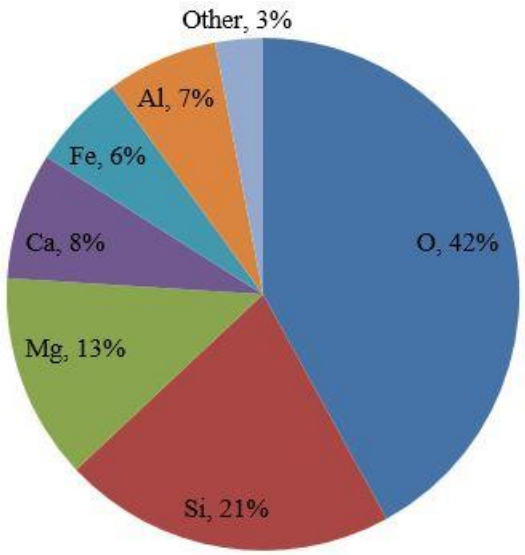

Figure 2. 2. Composition of Lunar Regolith [4]

2.4 Structural Concepts & Related Technologies

In the recent past, several structural concepts have been proposed for space and lunar habitats. Lunar habitat designs have advanced all through these years as the scientific prospects have changed. Some of the factors that need to be taken care of while designing a lunar structure are economic constraints, large variations in temperature, lack of atmosphere, higher levels of radiation, meteoroid strikes, and extended nights. The possibility of high radiation levels and meteoroid strikes increase with time. Hence, all structures must be able to mitigate radiation damage and meteoroid impacts. Below we review some of the proposed structural concepts.

In 1988, Vanderbilt proposed a pillow shaped structure for a permanent lunar base. Fiber composites along with quilted inflatable tensile structures are used in building this structure. To protect the lunar model from radiation, approximately 2.5 m to 3.0 m of regolith is positioned on top of the structure. Figure 2.3 shows the proposed inflatable structure.

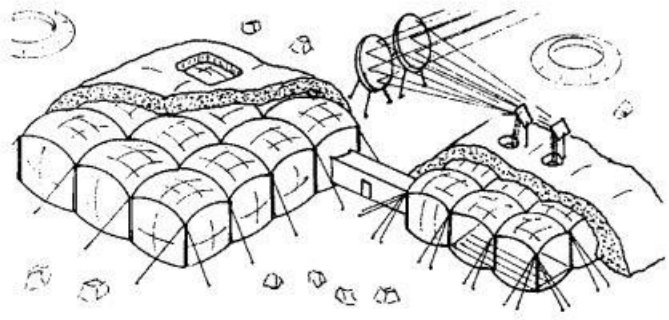

Figure 2. 3: Inflatable Structure Proposed by Vanderbilt in 1988 [6]

In 1988 and 1989, Chow and Lin proposed a double-skin pressurized membrane structure that is inflated with the help of structural foam. See Figure 2.4. Placing regolith on top of

the structure provides radiation shielding. Firstly, the ground is modified according to the shape of the structure, and the uninflated structure is placed upon it. Structural foam is then injected to hold the shape of the inflatable structure and the internal compartment is pressurized. To provide stability and flat surface, the bottom part of the inflated structure is filled with compacted soil.

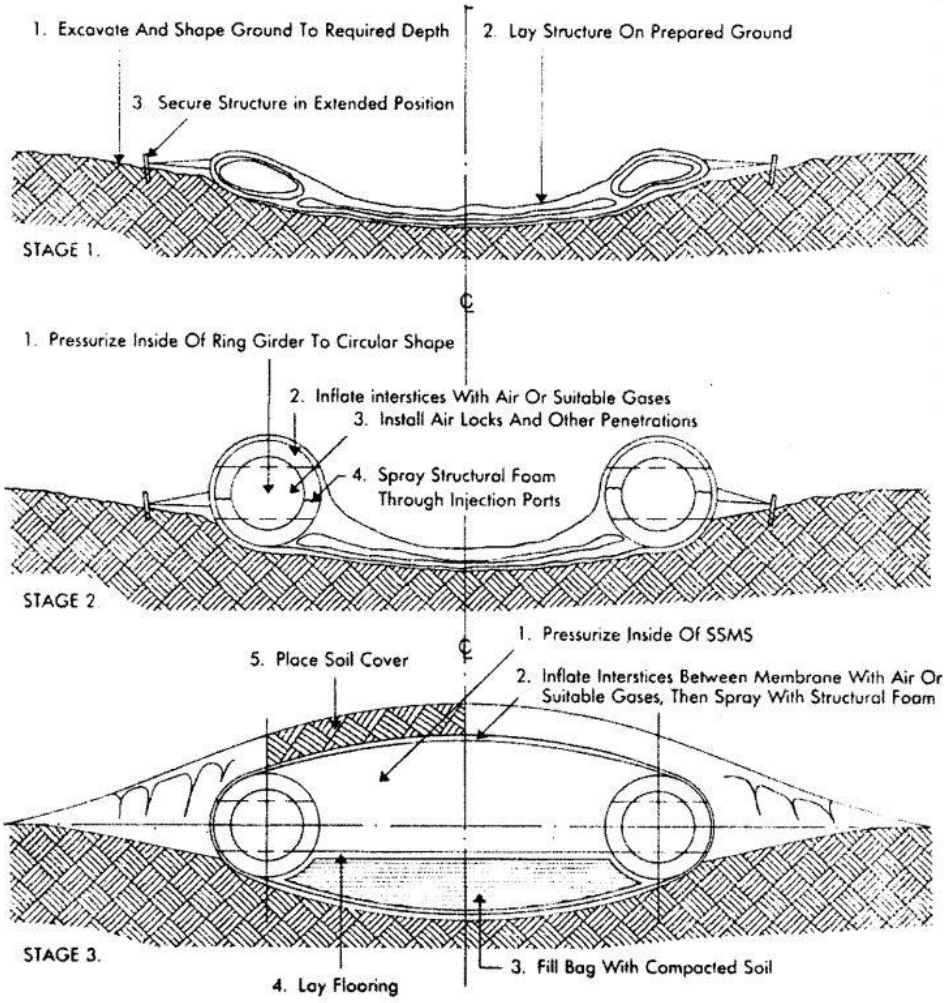

Figure 2. 4: Inflatable Membrane Structure – Construction Sequence by Chow & Lin [6]

2.4.1 TransHab

Another inflatable model suggested was the TransHab inflatable module for the International Space Station. The idea of TransHab was first initiated at NASA's Lyndon

B. Johnson Space Center, Houston, Texas, in 1997 as an alternate design for inflatable living quarters on forthcoming Mars-bound spacecraft. TransHab would be a unique hybrid structure that has load-bearing capabilities combined with packaging and mass efficiencies. Figure 2.5 shows the proposed TransHab configuration. TransHab is equipped with multiple layers of blanket insulation for protection from meteoroid strikes and radiation shielding. TransHab is shielded with nearly two dozen layers of Nextel, a commonly used insulation material, spaced between thick layers of open cell foam. Nextel combined with foam causes particles of space debris and meteoroids to break when they hit the shielding. The external layers or coatings protect several inner layers that are responsible for sealing the air in the module. The outer layers also protect from varying temperatures that can range from 121 ^{O}C in the day to -128 ^{O}C in the night. The inner layers are made of woven Kevlar fabric that holds the shape of the TransHab. The inner three layers are made of Combitherm, which is responsible for holding air inside it. The innermost layer is a Nomex cloth, which protects from fire and scratches.

The Central Structural Core is made of a lightweight carbon fiber material, and is a rigid structure that gives solid strength to the structure. It is an interface that provides three floors and partitions between compartments. There is center passageway that provides access to all levels. Protection is provided to middle level quarters in case of solar radiation storms with the help of a water storage tank enclosed around the level.

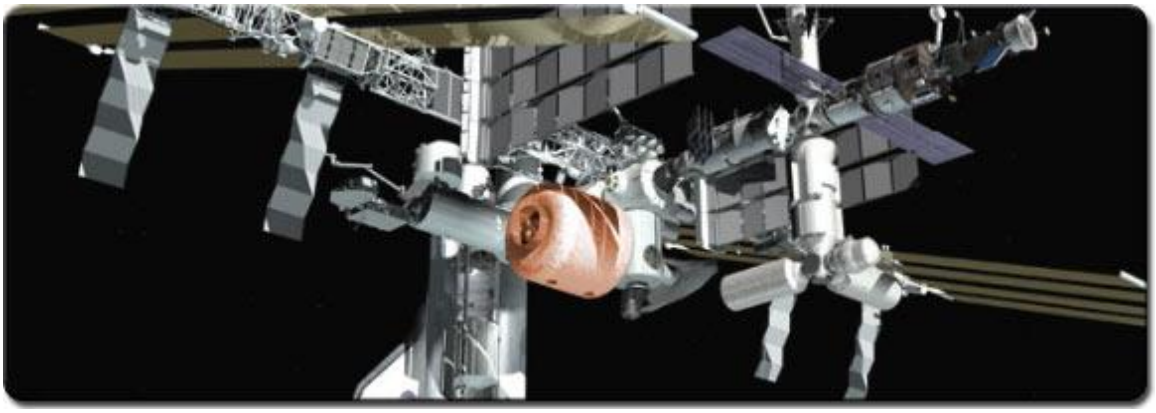

Figure 2. 5. Proposed TransHab Configuration on International Space Station [7]

2.4.2 Genesis I

Genesis I shown in Figure 2.6 was launched on 12 July 2006. The dimensions of Genesis I measure 4.4 m (14.4 ft) long and 2.54 m (8.3 ft) in diameter, with a habitable volume of 11.5 cubic meters (406.1 cu ft). Figure 2.6 shows the actual Genesis I. As it is an inflatable structure, the module was launched with a diameter of only 1.6 m (5.2 ft). Genesis I used a single gas tank for its inflation system. Genesis I suffered a solar storm in December 2006. [8] Although the avionics lifespan was only six months, Genesis I avionics worked impeccably well for over two and a half years before failure. [9]

Figure 2. 6. Image from one of the exterior cameras on Genesis I [8]

2.4.3 Expandable Lunar Habitat by ILC Dover

ILC Dover, in cooperation with NASA Johnson Space Center, has developed an expandable lunar habitat with two end caps and a deployable section at the center. The habitat packs into the end caps and doubles its length when deployed. NASA wanted to improve the inflatable structures technology because of its high strength-to-weight ratio and to decrease the weight carrying capacity of extra vehicular space units. The main idea of this prototype was to see how the inflatable structure reacts under constant load and pressure. The inflatable was 5.2 m long and would roughly double its length to 10 m when deployed. Using the Vectran fibers, they developed a webbing net construction system so that the inflatable would have a higher habitable volume and would be lighter

in weight when compared to its traditional metallic counterparts. Several layers of webbing with Vectran fabrics were used to get the required load capacity for the structure. The expandable habitat operated at an internal pressure of 9.0 psi and was expected to take 100 lb of force between webbings.

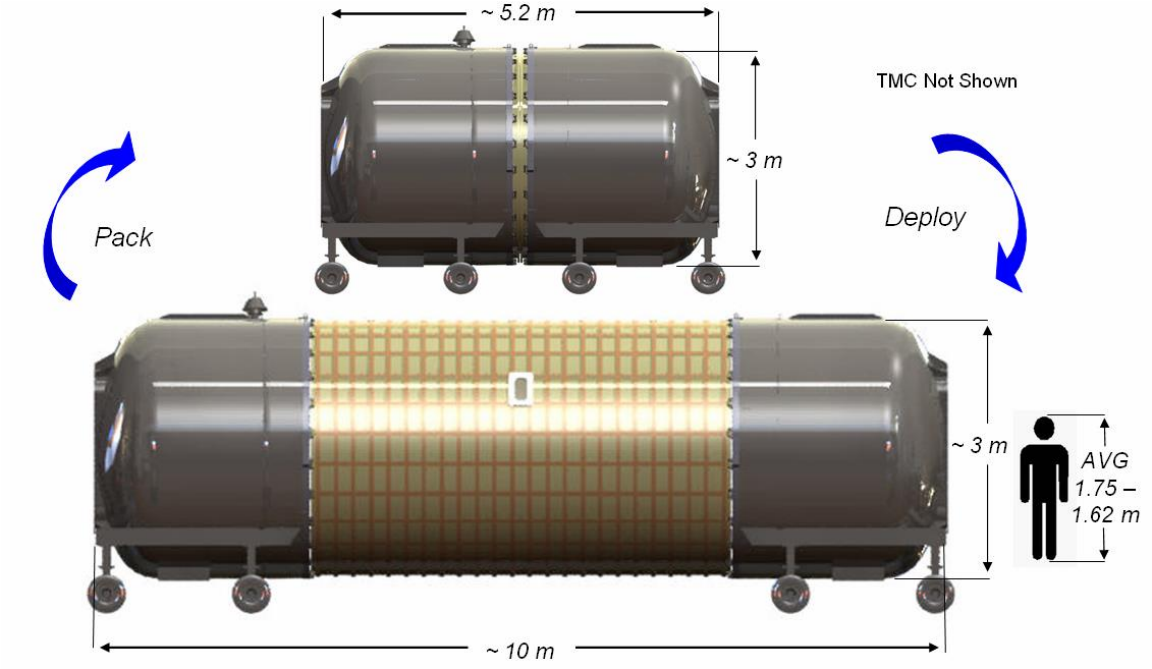

Figure 2. 7. Habitat deployed at ILC with test end caps installed [10]

2.5 Ongoing Research

Currently, ILC Dover, L'Garde, and Bigelow Aerospace are the three organizations leading in the field of inflatable space structures. Also, NASA is currently studying inflatable planetary habitats and airlock units. NASA has also collaborated with Bigelow Aerospace for space flight and International Space Station projects. Some of the significant research in this field is discussed below.

2.5.1 Bigelow Expandable Activity Module

The Bigelow Expandable Activity Module (BEAM) shown in Figure 2.8 is an experimental inflatable space station model developed under a NASA contract. It was launched on April 8th 2016 and was docked on April 16th 2016. It was inflated at the end of May, 2017, to test and validate inflatable habitat technology. It will serve as a significant entity for authenticating the benefits of expandable habitats. NASA is in the process of using this module for testing on International Space Station from 2016 – 2018. Table 2.4 shows the dimensions of the module in its packed and expanded state.

If BEAM can perform well, it could lead to the development of inflatable space structures for future interplanetary explorations. The main objectives of this mission are:

- To demonstrate launch and deployment techniques of the inflatable module and to find folding and packing efficiencies of inflatables.
- To determine radiation protection of the expandable model.
- To evaluate design performance of the structure, such as structural, thermal, mechanical durability and long term leak performance.
- To increase expandable habitat structure technology [11].

	Mass (kg)	Length (m)	Diameter (m)	Volume (m^3)
Packed	1400	2.16	2.36	3.6
Expanded	1400	4.01	3.23	16

Table 2. 4. Specifications of BEAM [11]

Figure 2. 8. Bigelow Expandable Activity Module [11]

As of 2013, Bigelow Aerospace is trying to build second BEAM to use as an airlock on its Bigelow Commercial Space Station.

2.6 Locations

While some hazards are constant throughout the lunar surface, the intensity of hazards changes from place to place. So, we first look at a possible location for our structure, gather all the parameters, and apply the appropriate design.

Several important criteria that are considered, before choosing a location for lunar outpost, are:

- It should have good transportation conditions.
- It should feature different types of scientific interests of the Moon.
- The location should be rich in natural resources, such as oxygen, and water.

There are two broad categories for a location on the Moon. They are the polar regions, and the equatorial regions.

2.6.1 Polar Regions

The two poles of Moon, the North Pole and the South Pole, might be attractive locations for a lunar base, as there is evidence that water may be present in some continuously shaded areas near the poles [12]. Also, power collection stations could be located so that they are exposed to continuous sunlight because of the Moon's axis of rotation. As a result of uneven surfaces on the Moon, some areas have almost uninterrupted sunlight [13].

2.6.2 Equatorial Regions

Equatorial regions have an advantage for launching material due to the slow rotation of Moon where the orbit nearly coincides with equatorial plane of the Earth. These regions are rich in concentrations of Helium-3 because of the high angle of incidence of solar wind. The Helium-3 can be a fuel for an eventual nuclear fusion reactor. Several missions, like Apollo 12, have landed in the Oceanus Procellarum area and there are many more areas that could be studied for long-term uses [14].

Taking the above criteria into consideration, Shackleton crater, a region at the South Pole, would be a better fit for a lunar base, keeping in mind the frozen water, oxygen, and continuous sunlight, which are essential for a human colony.

Various parameters of Shackleton crater are given in Table 2.5.

Radius of circular rim	10.5 km
Radius of floor	3.3 km
Depth	4.2 km
Loss rate of any ice by vaporization at 90 K	10^{-26} to 10^{-27} m/s

Maximum temperature of floor at center	-88 K
The hemispherical visual albedo around the center	0.23 ± 0.05
Crater volume	640 ± 10 km^3
Maximum wall slope	35^0
Average wall slope	30.5^0

Table 2. 5. Parameters of Shackleton crater [15]

Chapter 3. Material Selection

As discussed in the literature review chapter, there are many materials to consider before making a selection for the structure. As discussed earlier our design consists of two parts. The upper part is the main inflatable structure that is transported to the Moon and inflated there. For the foundation base upon which the inflatable will sit, we consider materials that are abundantly available on the Moon, and can be easily machined or prototyped on the lunar surface, as it's not economically feasible to transport the full foundation base from Earth. In this chapter, we explore possible materials for the inflatable structure, and the foundation base that are available and feasible to build on lunar surface.

3.1. Kevlar for Inflatable Structure

Kevlar is a high-strength para-aramid synthetic fiber developed by Kwolek at DuPont in 1965 [16] that was first commercially used in the early 70's in racing tires. In the recent past, Kevlar has become an important composite material used for numerous applications, from building kayaks and aircraft parts, to making ballistic panels and bulletproof vests. While there are several grades of Kevlar, the most common types are Kevlar 29 and Kevlar 49.

3.1.1 Kevlar 29 vs. Kevlar 49

Kevlar 29 fabrics are generally built for ballistic applications. They have a high strength-to-weight ratio and can withstand high-speed impacts. They can withstand a great deal of energy before breaking. This is the reason they are used to make bulletproof vests. Kevlar 29 can also withstand high temperatures and harsh environments.

On the other hand, Kevlar 49 is most commonly used in boats and the aerospace industry. It has higher resistance to torque and tensile stresses. This material is generally used in building boats and fighter jets. Eurofighter is one fighter jet that is built with Kevlar 49 and can survive small arms fire. This fighter jet is more agile as compared to traditional jets because of the low weight and high strength property of Kevlar 49 [17].

Since our structure is built for usage on the Moon, and we consider meteoroid impacts in our design criteria, we select Kevlar 29, which has more resistance to impacts and can withstand higher kinetic energies. The elongation at break for Kevlar 29 is 3.6% as compared to 2.4% for Kevlar 49, which indicates Kevlar 29 has more resistance to shape changes.

We look at some of the properties of Kevlar 29 as compared to Kevlar 49 in Table 3.1.

Property	Units	Kevlar 29	Kevlar 49
Density	g/cc	1.44	1.44
Young's modulus	MPa	70500	112,400
Tensile Yield Strength	MPa	2920	3000
Poisson's Ratio	-	0.36	0.36
Tensile Ultimate Strength	MPa	3600	3600
Elongation at Break	%	3.6	2.4

Table 3. 1. Properties of Kevlar 29 [18]

3.1.2. Advantages of Kevlar

Kevlar is most famous for its low weight and high strength properties. For example, the density of Kevlar is almost half the density of glass (S or E) but Kevlar's tensile modulus

is approximately the same. Kevlar, when combined with other materials like a composite, is very stable at high temperatures as it has a slightly negative coefficient of thermal expansion, like graphite. But unlike graphite, Kevlar is very resistant to abrasion and impact damages, and is often used as fire resistant clothing and scratchproof gloves. Also, Kevlar is more flexible if it is combined with rubber, making it even stronger during high-speed impacts. It is used in making racing car petrol tanks, as the light weight of Kevlar helps in reducing the weight of the vehicle and its flexibility helps in surviving collisions at high speed, avoiding explosions. Table 3.2 shows properties of Kevlar 29 and Kevlar 49 when compared to other yarns.

	"Customary" (inch-pound) Units							
	Specific Density lb/in.^{3}	Tenacity 10^3 psi	Modulus 10^6 psi	Break Elongation %	Specific Tensile Strength* 10^6 in.	CTE** 10^{-6}/°F	Decomposition Temperature °F	(°C)
KEVLAR 29	0.052	424	10.2	3.6	8.15	-2.2	800-900	(427-482)
KEVLAR 49	0.052	435	16.3	2.4	8.37	-2.7	800-900	(427-482)
Other Yarns								
S-Glass	0.090	665	12.4	5.4	7.40	+1.7	1,562†	(850)
E-Glass	0.092	500	10.5	4.8	5.43	+1.6	1,346†	(730)
Steel Wire	0.280	285	29	2.0	1.0	+3.7	2,732†	(1,500)
Nylon-66	0.042	143	0.8	18.3	3.40	—	490†	(254)
Polyester	0.050	168	2.0	14.5	3.36	—	493†	(256)
HS Polyethylene	0.035	375	17	3.5	10.7	—	300†	(149)
High-Tenacity Carbon	0.065	450	32	1.4	6.93	-0.1	6,332	(3,500)

*Specific tensile strength is obtained by dividing the tenacity by the density.

**CTE is the coefficient of thermal expansion (in the longitudinal direction).

†Melt temperature.

Table 3. 2. Comparison of properties of Kevlar with other yarns [18]

3.1.3 Disadvantages of Kevlar

The biggest disadvantage with Kevlar is that it tends to absorb moisture and is more sensitive to the environment when compared with glass or graphite. To overcome this, Kevlar is generally combined with moisture resistant materials. Although, Kevlar has high tensile strength, it has relatively poor compressive properties. Laminated Kevlar is

difficult to machine and also very difficult to cut and shape unless we use special cutters and equipment. Also, Kevlar should be protected from direct sunlight, as it reacts badly to UV light (sunlight). Kevlar, when exposed to chlorine, suffers some corrosion.

3.2 Magnesium as Base Material

The primary criterion for selecting the foundation base material is that it should be abundantly available on the lunar surface so that it can be fabricated on the Moon. From Figure 2.2, we can see that magnesium is abundantly available in the lunar environment. We next look at some of the advantages and disadvantages of magnesium as compared to other metals.

3.2.1 Advantages of Magnesium

Magnesium has a low melting temperature of 650 ± 2 ˚C so that it can be produced and recycled by heating it in furnaces on the lunar surface. [19, 20] Also, producing magnesium is less expensive when compared to other metals like aluminum, iron or titanium, which have melting points at 660 ˚C, 1535 ˚C and 1795 ˚C, respectively. Table 3.3 summarizes the comparison of properties of magnesium with other metals.

	Specific gravity	Melting Point (˚C)	Boiling point (˚C)	Latent Heat of melting (kJ/kg, J/cm^3)	Specific heat (kJ/kg.K, J/cm^3.K)	Coefficient of linear expansion × 10^6	Tensile strength (MPa)	Elongation	Hard-ness (HB)
Mg	1.74	650	1110	368, 640	1.05, 1.84	25.5	98	5	30
Al	2.74	660	2486	398, 1088	0.88, 2.43	23.9	88	45	23
Fe	7.86	1535	2754	272, 213	0.46, 3.68	11.7	265	45	67
Ti	4.54	1795	3287	419, –	0.54, –	8.6	434	18	72

Table 3. 3. Comparison of Properties of Magnesium with Other Metals [21]

When it comes to machinability, magnesium is one of the most easily machined metals [22, 23] and has excellent castability [24-26], which makes it easy to work with CNC (Computer Numerical Control) machines, decreasing the dependency on Earth-based manufacturing.

Magnesium alloys have high strength-to-weight ratios, especially in alloys like AZ91, which outperforms steel [22]. With the recent advances in technology, magnesium alloys have been shown to have stronger mechanical properties than aluminum and steel [27]. Recently, usage of magnesium alloys in aerospace and automotive applications have been increasing rapidly because of its low weight and high strength properties. Properties of magnesium can be seen in Table 3.4.

Magnesium and aluminum are considered to be the radiation shielding materials of choice for space applications because of their relative conductivities of 0.36 and 0.61, respectively [28, 29]. Due to its conductivity and permeability, magnesium exhibits strong electromagnetic shielding properties. Magnesium has high impact resistance [21, 30] and also has 30 times the vibrational damping of aluminum [24], which is helpful during meteoroid impacts and moonquakes.

3.2.2 Disadvantages of Magnesium

One of the main disadvantages of magnesium is its highly reactive nature with water and oxygen. However, because of the lack of atmosphere on the Moon, this is not a problem if magnesium is used on external surfaces. For the internal surfaces, we assume the entire magnesium structure is sealed from inside and also the alloys like AZ 91 are more resistant to corrosion when compared to traditional magnesium alloys.

As the Moon's gravity is one-sixth of the Earth's gravity, the lower tensile strength and fatigue strength of magnesium as compared to aluminum and other metals [24] become less important. Also, the tensile strength can be improved by using stronger magnesium alloys (produced by Elektron Ltd.).

The refining process of magnesium is expensive as the separation of MgO from regolith is difficult. We have some proposed indirect methods for the extraction [19, 20, 31, 32] but there is no study focused directly on refining magnesium on the lunar surface. Also, magnesium and its alloys are highly flammable in their pure, powder or ribbon form. This ignition safety risk is drastically reduced due to the lack of atmosphere on the Moon, yet there is a chance of presence of oxygen during the refining processes of regolith for magnesium. Studies have shown that by adding calcium, the ignition point of magnesium alloys can be raised by 200 – 300 ˚C [21].

Property	Units	Value
Tensile Yield Strength	MPa	150
Compressive Yield Strength	MPa	165
Ultimate Tensile Strength	MPa	230
Coefficient of Thermal Expansion, 20˚C	µm/m-˚C	25
Density	g/cm^3	1.81
Poisson's ratio	-	0.35
Young's Modulus	GPa	45

Table 3. 4. Properties of Magnesium Alloy AZ91D [33]

Chapter 4. Static Analysis and Design Configurations

The geometry of the lunar structure considered here is based on the TransHab concept. The lunar structure that we are analyzing is for six astronauts, and is being designed by considering Kevlar fabric as the material for the main inflatable structure and magnesium for the foundation base. We start the design of the structure based on the criteria of minimum habitable volume required per person, and then build the model eventually with an appropriate factor of safety. Then, Solidworks is used to draw the CAD model of the lunar structure, and ANSYS® Workbench (academic version), release 14.5, is used to conduct the finite element analysis to verify the resistance of the structure to the environmental loads.

4.1 Overview of the Lunar Structure

The review of the earlier lunar structural designs in the literature review suggests that an inflatable structure be selected because of its high strength-to-weight ratio and low transportation costs. Our design consists of two parts, with the upper inflatable part being the main living area for the astronauts, and the lower rigid part being the foundation base that includes a doorway and is used for storage and processes. We also have an elevator for the astronauts to travel from the inflatable structure to the base. In the following sections, we further discuss the design and the choice of appropriate materials.

This design is meant to take advantage of the benefits of both inflatable structures and rigid structures. The base may be fabricated on-site via robotic, layered manufacturing. The inflatable part can be sent from Earth and attached in a relatively simple way, as described in the sections below.

4.2 Habitable Volume Per Person

Based on the parameters defined in Mars DRM 5.0 and research conducted at NASA, the minimum acceptable habitable volume is 25 m^3 (883 ft^3) per person [34]. As discussed earlier, the semi-rigid structure is for six astronauts, that is, we are looking at a minimum habitable volume of about 150 m^3 (5298 ft^3). This amount of habitable volume is the minimum we need for six people, but we can actually consider having more volume to whatever extent we may want. Considering the economic costs and the building capabilities on the Moon, we consider a conservative design with 200 m^3 (7064 ft^3) of habitable volume. We consider a dome-like structure with a foundation base of radius 15 ft, thus providing 200 m^3 (7064 ft^3) of habitable volume after the entire structure is constructed.

4.3 Inflatable Structure

As discussed in earlier sections, inflatable structures have many advantages as compared to the traditional rigid structures. Inflatable structures are more economical to transport from Earth to the lunar surface and have high strength-to-weight ratios after inflated. We consider designing a two-layered semispherical inflatable structure with a radius of 15 ft (180 in) and a height of 10.83 ft (130 in). By symmetry, it will nominally have equal magnitudes of stresses in every direction – although there can be slight asymmetries – so that one or two areas of high stress concentrations do not affect the entire structure.

We consider two layers of 0.16 ft (2 in) thickness with a gap of 0.16 ft (2 in) between them, which holds the inflatable structure rigid when inflated. Inflating the structure by air is one of the most common methods, which requires a number of layers within the structure to be puncture resistant and strong enough to hold the air pressure. Rather, we

try to inflate the structure by filling the gap of 0.16 ft (2in) with epoxy as it becomes rigid ones it comes out and can act as puncture resistant to the structure. Properties of epoxy can be seen in Table 4.1.

Property	Units	Value
Young's Modulus	MPa	64.8
Tensile Yield Strength	MPa	50
Tensile Ultimate Strength	MPa	692
Density	Kg/m^3	1250
Poisson's Ratio	-	0.3

Table 4. 1. Properties of Epoxy

4.4 Base Structure

As we are using Kevlar fabric for the inflatable, we don't want to insert doorways in the fabric that will result in a high stress concentration area. Also it would be difficult to sustain the internal pressure with repeated openings of the door. Instead of making it on Earth and transporting it to the Moon, increasing the cost of transportation, we propose to make the magnesium support base on the lunar surface assuming we have necessary machinery available for the excavation. Ideally, we are able to send autonomous 3D printing robots that can extract and process the surface magnesium and create the base for the inflatable portion of the habitat. The base has the same dimension as inflatable of 30 ft diameter with a total height of 9.6 ft (116 in). This base has the doorway for exit to the lunar surface, and an elevator by which astronauts move from base to inflatable. It can also be used as a storage compartment as it has a volume of 5024 ft^3 (142 m^3).

4.5 Regolith Shielding

We start designing the structure by considering the extreme temperatures and radiation levels on the Moon. In order to protect the astronauts from those radiation levels and extreme temperatures we place lunar regolith (which is abundantly available on lunar surface) around and on top of the surface of the structure. The shielding regolith layer around the structure should be thick enough to not let the extreme temperatures touch the Kevlar fabric. Previous studies suggest that a 2 m (6.56 ft) or 3 m (9.84 ft) thick regolith layer can protect the module against the extreme temperatures of about 253 °F at day and -243 °F at night [4, 35]. We choose a 3 m thick regolith layer for the initial calculations and modify the thickness, if necessary, depending upon the results obtained from finite element analysis. Properties of regolith can be seen in Table 4.2.

Property	Unit	Value
Tensile Strength	MPa	34.5
Compressive Strength	MPa	538
Young's Modulus	MPa	100000
Poisson's Ratio	-	0.28
Density	Kg/m^3	1500

Table 4. 2. Properties of Cast Regolith [36, 37]

4.6 Aluminum Plate

We have the two parts of our structure modeled above. Now we have the challenge of fitting them together. We cannot directly bolt down the fabric to the magnesium base as it creates a high stress concentration factor and may result in tearing the fabric apart. In order to fit them together we consider using an aluminum plate where the Kevlar is

tucked in between the plate and base. Also, the fabric is made in such a way that it has gaps for the bolts. Figures 4.1 and 4.2 provide sketches of the concept. Also, we choose aluminum as fastener material as the regular carbon alloy fasteners might react with magnesium creating the galvanizing effect. Table 4.3 presents the properties of aluminum.

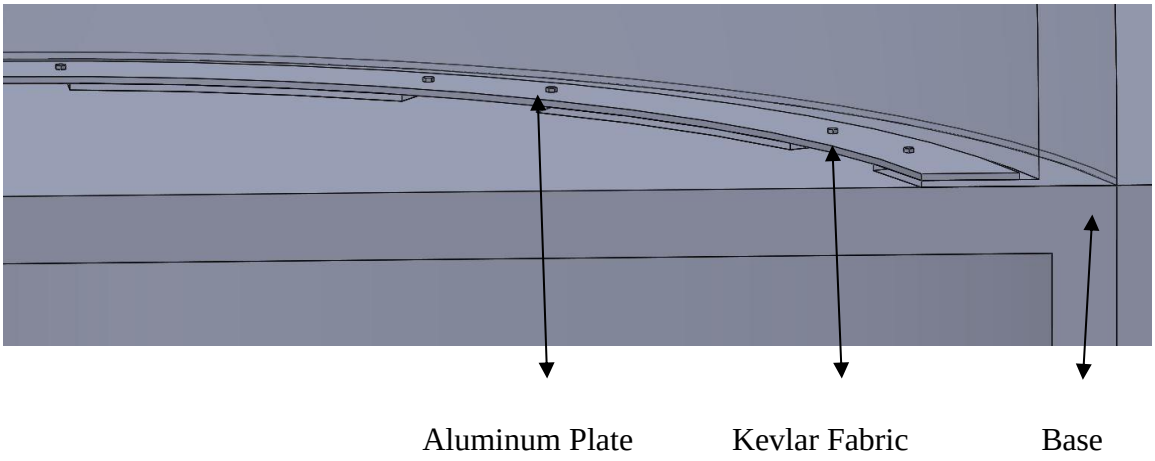

Figure 4. 1. Kevlar fabric in between plate and the magnesium base

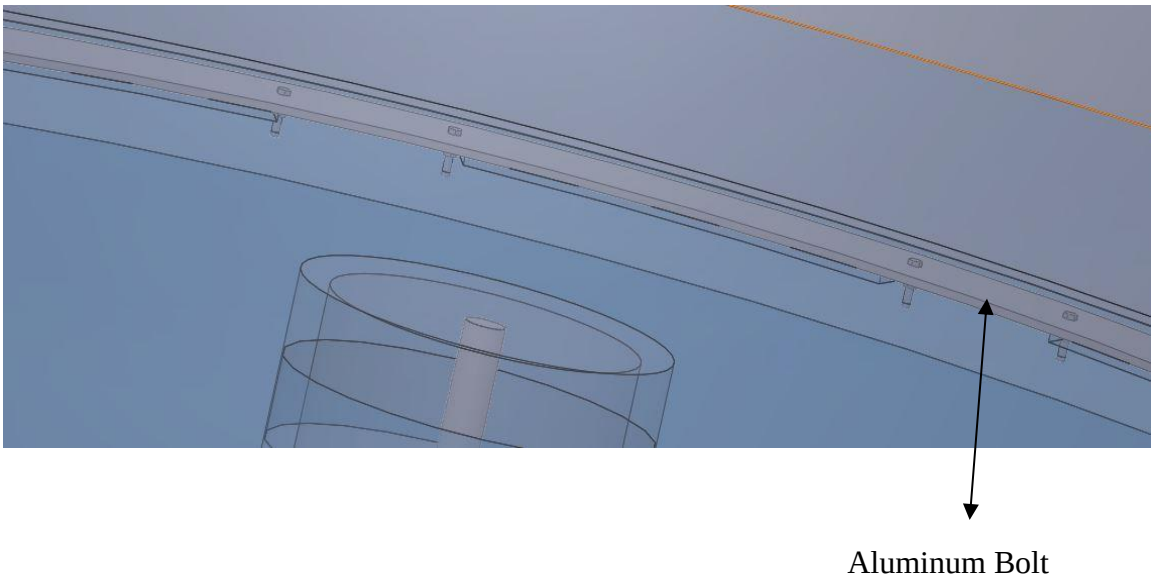

Figure 4. 2. Bolting down the Kevlar to base

Property	Units	Value
Density	g/cm^3	2.7
Tensile Yield Strength	MPa	276
Ultimate Tensile Strength	MPa	310
Coefficient of Thermal Expansion, linear 250°C	µm/m-°C	25.2
Young's Modulus	GPa	68.9
Poisson's Ratio	-	0.33

Table 4. 3. Properties of Aluminum

4.7 CAD Model

SolidWorks is used to draw the parts and then the assembly feature is used to assemble multiple parts into one solid model. As discussed, the base is drawn with a radius of 15 ft (180 in) and a wall thickness of 0.16 ft (2 in). This is essentially a thin walled pressure vessel ($t/r \leq 0.1$). The thin walls in tension are more resistant to bending. The entire dimensions of the base and fabric, and the engineering drawing, are presented in Figures 4.3, 4.4 and 4.5. All dimensions are in inches. The CAD model of the structure can be seen in Figure 4.6.

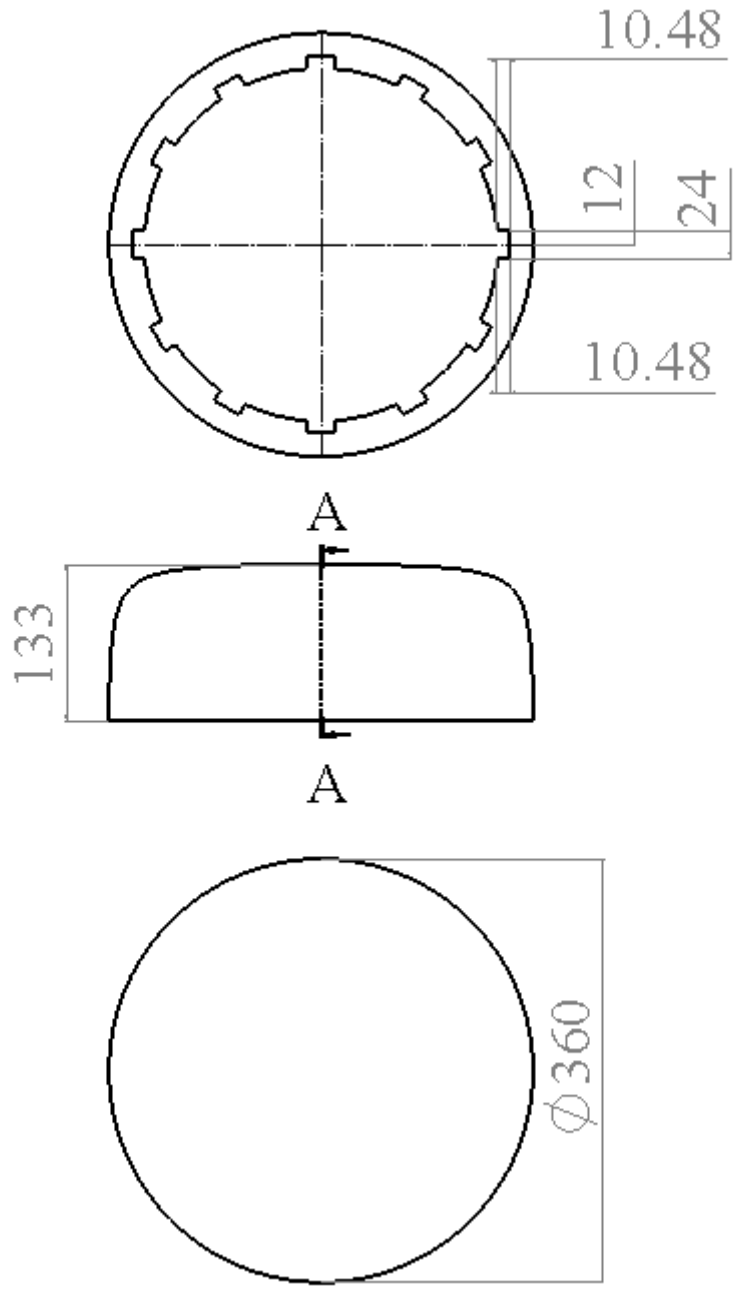

Figure 4. 3. Dimensions of inflatable structure

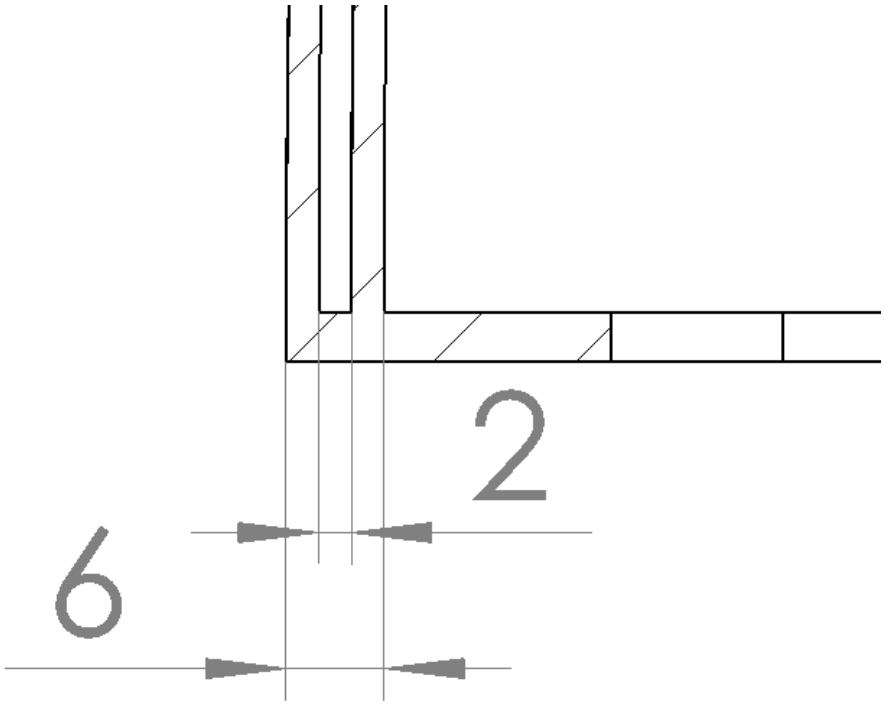

Figure 4. 4. Dimensions for wall thickness of Kevlar and thickness of Epoxy.

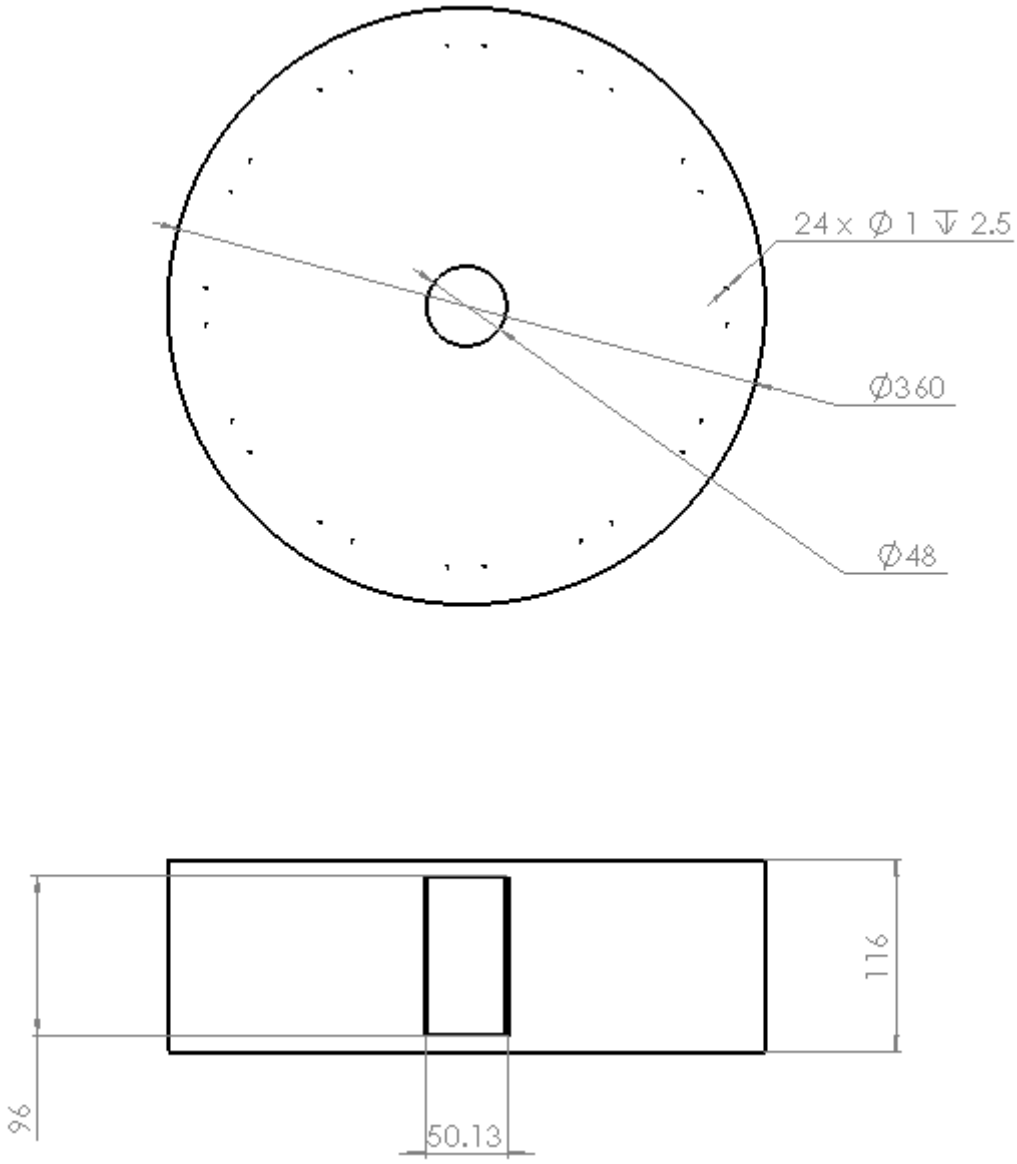

Figure 4. 5. Dimensions of Magnesium Base

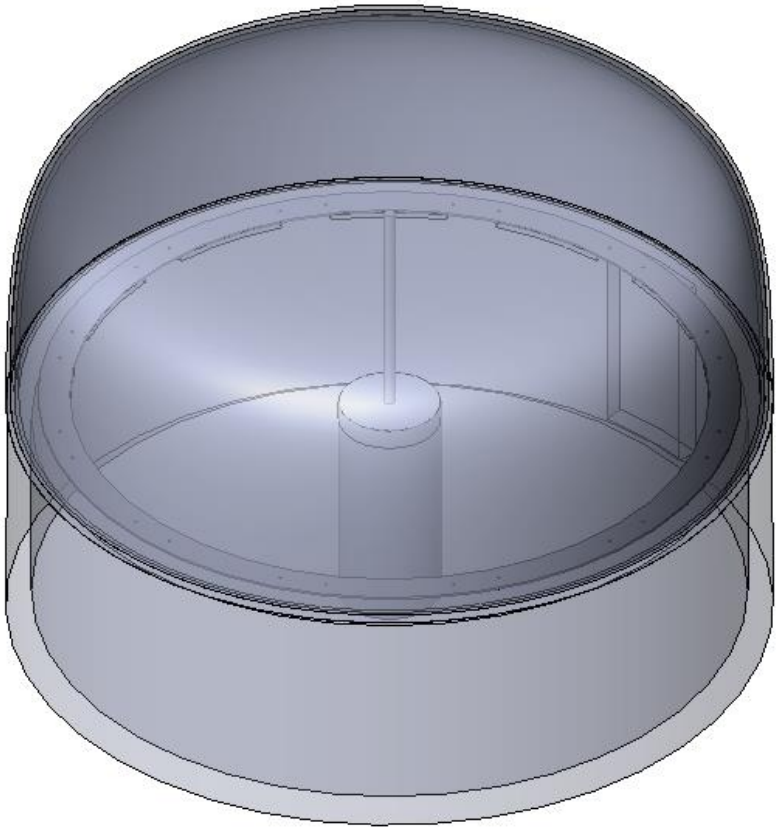

Figure 4. 6. CAD model of the complete structure

4.8 Finite Element Analysis

ANSYS® Workbench (student version) is used for the finite element analysis. We start the analysis by considering the lunar structure to be fixed to the lunar surface. All interior surfaces of the Kevlar inflatable structure are subjected to a uniform internal pressure of 101.35 KPa (14.7 psi). The 3 m regolith shielding placed on the structure has a bulk density of 1500 kg/m^3 [4, 37], which results in a uniform downward pressure of 44.05 KPa (6.39 psi). A negative acceleration of 1.63 m/s^2 (1/6th of Earth's gravitational force) is taken for the lunar gravitational force. The properties of Kevlar and magnesium are given as discussed in the materials section.

Static Structural analysis in ANSYS academic version is used to run the load simulations. A triangular mesh was generated with 132,653 nodes and 88,453 elements. The generated elements are SOLID 187 and SOLID 186 type.

SOLID 187:

SOLID 187 element is a 3D, 10-node element. This element is capable of modeling plasticity, hyper elasticity, creep, stress stiffening, large deflection and large strain. It is well suited for modeling irregular meshes and has a quadratic displacement behavior.

SOLID 186:

SOLID 186 is a 3D, 20-node element. It has the same capabilities as of SOLID 187 element and has a quadratic displacement behavior. It is suitable for modeling irregular meshes.

The results for the static loading analysis can be seen in Figures 4.7, 4.8, 4.9, 4.10.

4.9 Analytical Calculations

From Figure 4.8, we have the maximum equivalent stress of 12.35 MPa acting on the structure, which is calculated by using ANSYS. We also want to order-of-magnitude calculate the stress acting on the structure analytically in order to be confident with the ANSYS results.

Our inflatable structure is designed in the shape of a hemisphere, and for a hemisphere the stress acting in every direction is the same. The stress is approximated by Eq 4.1 to calculate stress acting on hemisphere.

$\sigma = \frac{P \times D}{4t}$ where, Eq 4.1.

D = Internal diameter of structure = 348 in

P = internal pressure = 14.7 psi

t = Wall thickness = 4 in

σ = Allowable stress

σ = 319.725 psi = 2.20 MPa

The calculated theoretical stress of 2.2 MPa, and the respective stress of 12.35 MPa results from the ANSYS simulations.

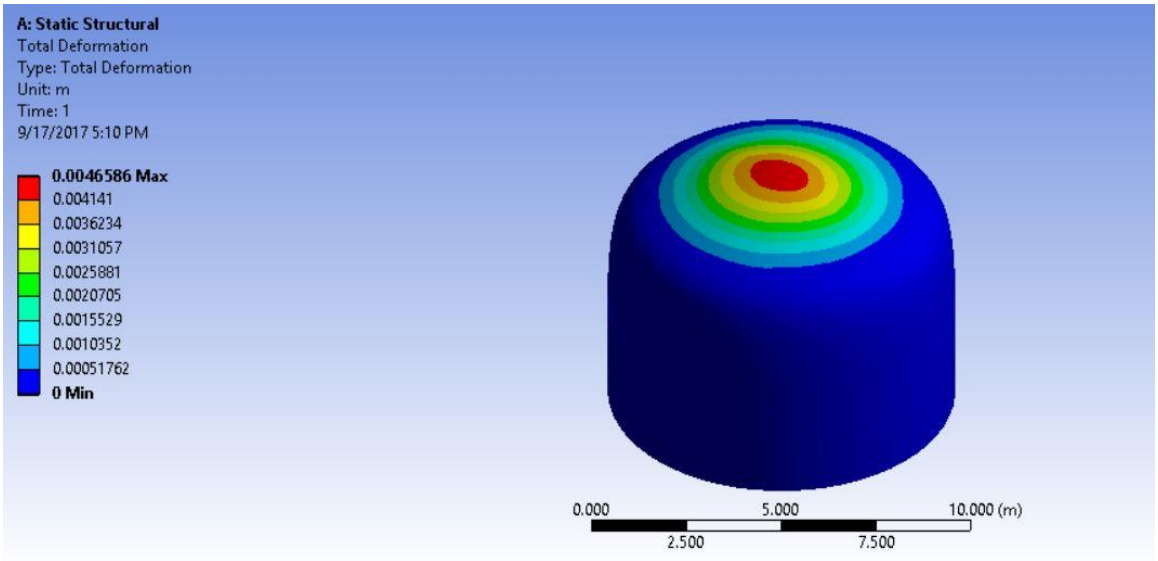

Figure 4. 7. Total deformation

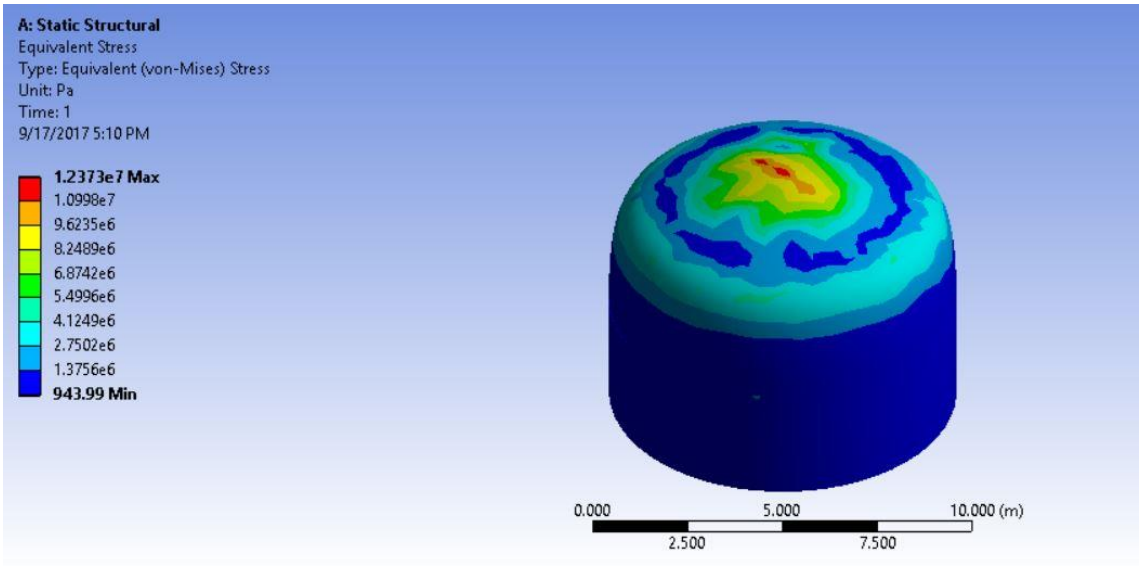

Figure 4. 8. Equivalent stress

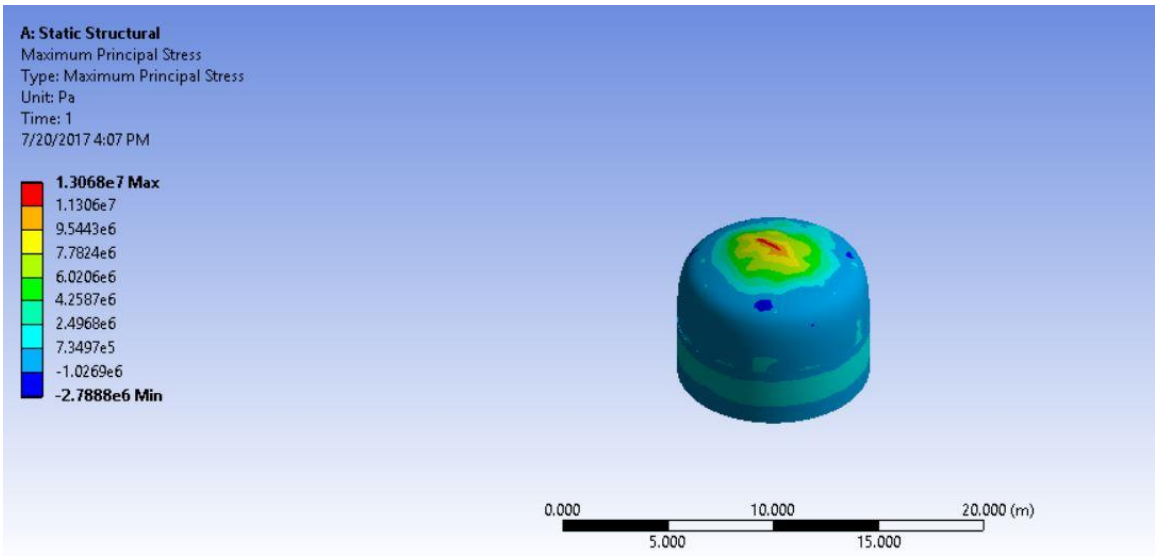

Figure 4. 9. Maximum principal stress

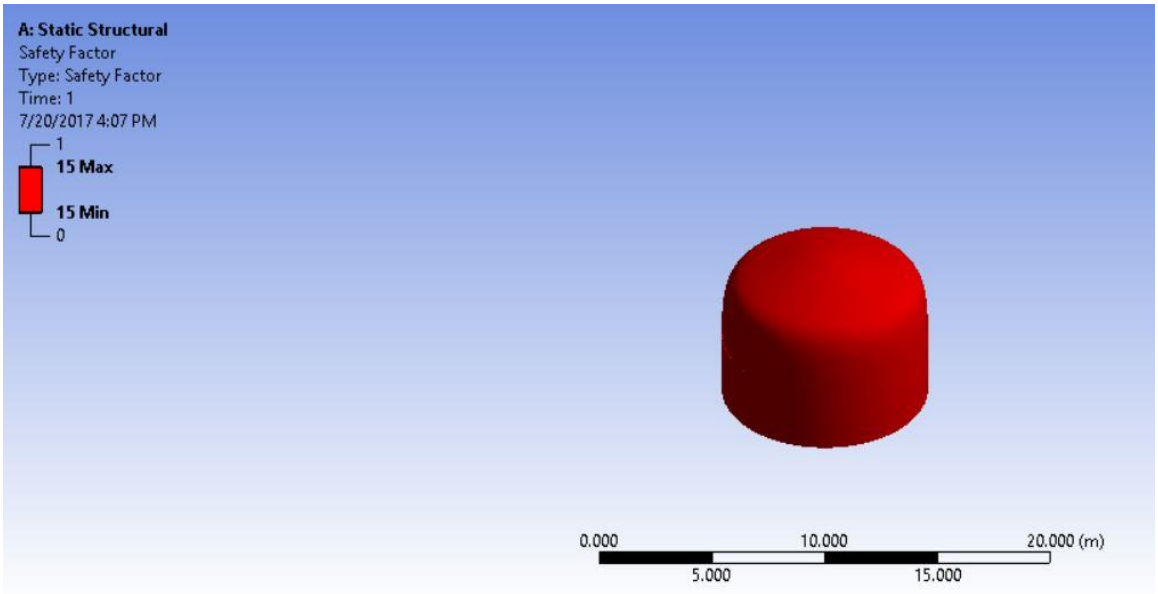

Figure 4. 10. Factor of Safety

4.10 Discussion

From Figures 4.7 and 4.8, we observe that the maximum deformation of the structure is 4.6 mm, which is almost negligible when compared to the strength of the material. Also, the maximum equivalent stress acting on the structure is 12.37 MPa, which is much lower than the yield strength of Kevlar at 2920 MPa. Figure 4.10 shows that the factor of safety of the structure is 15, which is acceptable for structures in the space and lunar environment, at this early stage of development [10].

From the analytical calculations in Section 4.9, we can see that the maximum stress is 2.2 MPa, which is an order of magnitude smaller than the maximum stress obtained from ANSYS simulations. While the very simplified stress equation does not adequately represent the actual stress, it does give us some confidence in the simulation results.

Chapter 5. Meteoroid Impacts and Lunar Dust

Apart from solar radiation, threats of structural failure on the lunar surface are due to lunar dust, and meteoroid impacts. (We call the tiniest particles dust.) As the impacts of very large meteoroids occurs infrequently, and we cannot design the structure to withstand large meteoroid impacts, we only consider meteoroids or lunar dust impacts for a range of radii of 1 mm to several mm, increasing the radii till the structure fails. We are interested in making a first-order approximation of the effect a meteoroid impact could have on the structure analyzed here.

5.1 Properties of Meteoroids

Meteoroids are of several types with several different compositions of materials. The most common type of meteoroid or lunar dust is made mostly of rocks. Meteoroids generally travel at speeds of 3.5 km/s to a maximum of 72 km/s, but due to the pulverization of materials starting at speeds of 6 km/s, we only consider speeds less than 6 km/s. Also, meteoroid densities range from 0.5 g/cc to 7.8 g/cc, depending on meteoroid composition. As most meteoroids are made of rocks, and also the large meteoroids are very rare, we consider meteoroids of density 1.5 g/cc. Properties of meteoroids that we consider are given in Table 5.1.

Property	Unit	Values
Young's Modulus	GPa	25
Density	g/cc	1.5
Velocity	km/s	5.5

Table 5. 1. Properties of Meteoroids

5.2 Impact Force on Structure

ANSYS academic version limits the possibility to run the dynamic stress simulations on the structure at the time of impact. So we assume the following energy equivalence in order to estimate how the structure and regolith shielding will deform, while absorbing all the energy of the impacting meteoroid. We realize that this is a crude approximation. We consider the kinetic energy and work done by the meteoroid at impact in order to find the impact force on the structure, and take that as our input for the static load simulations. Empirical equations are available that relate the energy to the displacement. Then, we can find the force, which is used as input to our computational model.

The kinetic energy of the meteoroid, and the work done during the impact of the meteoroid onto the regolith shielding and the structure, are

$$E_m = \frac{1}{2} mv^2$$

$$W = F * h.$$

We assume that at impact, the entire kinetic energy of the meteoroid is converted into work done on the structure. Therefore,

$$E_m = W$$

$$F = \frac{mv^2}{2*h}, \qquad \text{Eq.5.1}$$

where E_m = energy of meteoroid, W = work done at the time of impact,

m = mass of the meteoroid in grams equals ρ * Vol,

v = velocity of meteoroid in km/s, and

F = force acting on structure at the time of impact.

5.3 Displacement and Force Calculations

As we discussed earlier, we start the analysis by assuming a meteoroid of radius 1 mm. Then,

Volume of meteoroid = Vol = $4\pi\frac{r^3}{3}$ = 0.00419 cc

Mass of meteoroid = ρ * Vol = 0.0062 g

To determine the displacement of the structure resulting from the meteoroid impact, we use Eq 5.2 [38]:

$$hE^{0.243} - 384.79\,[mv^2 - 0.013466\,h_s v m^{5/6} \rho_p^{-1/3} - 0.3048\,mv]^{1/3} > 0. \qquad \text{Eq 5.2}$$

In the above equation, it is assumed that the energy required to penetrate the structure is the total energy of the meteoroid less than the energy required to penetrate the regolith, which results in the negative terms within the brackets. We also assume that there are no interactions between the interfaces at the time of impact. This equation is made for lunar structures considering the parameters on lunar surface.

The following are the variables,

h = displacement of the structure in mm, h_s = Depth of regolith in mm,

ρ_p = Projectile density of meteoroid in g/cc. E = Young's Modulus of target in kPa,

From the properties of the meteoroid and regolith shielding, as discussed in the earlier sections, we have

$\rho_p = 1.5$ g/cc $\qquad$ $E = 25 * 10^6$ kPa

$h_s = 3$ m $= 3000$ mm $\qquad$ $v = 5.5$ km/s.

By substituting the above values into Eq 5.2, we find the displacement of the structure due to the meteoroid impact, as follows,

$$h\,(25 * 10^6)^{0.243} - 384.79[(0.0062 * 5.5^2) - 0.013466(3000)(5.5)(0.0062^{5/6}) - 0.3048(0.0062)(5.5)]^{1/3} > 0$$

$$h\,(62.7623) - 384.79[0.1875 - 3.2140 - 0.0571]^{1/3} > 0$$

$$h\,(62.7623) + (560.0710) > 0$$

$$h > 8.92 \text{ mm}.$$

Substituting h = 9 mm into Eq 5.1, we find an first-order approximation of the force of impact,

$$F = \frac{0.0000062 * (5500)^2}{2 * (0.009)}$$

$$F = 10.419 \text{ kN}.$$

This force is taken to be the impact force on the regolith/structure, and is used to find the resulting displacement at the region of impact.

5.4 ANSYS Stress Strain Simulations

Taking the above force as a meteoroid impact load on the regolith, we run the stress strain simulations on the structure through ANSYS, with the results shown below in Figures 5.1, 5.2, 5.3, 5.4 and 5.5. These are discussed subsequent to the study of the max force, and max meteoroid radius that the structure can sustain.

5.5 Maximum Force on Structure

From above simulations, we know that the structure can sustain meteoroids with radii smaller than 1mm, but the question is, what is the maximum size of meteoroid the structure can sustain?

We use stress equations to find out the maximum force our structure can sustain,

$$\text{Stress} = \frac{Force}{Area}$$

Surface Area of Semi sphere = $2\pi r^2$ m^2

We know that the diameter of the regolith shielding is 15.143 m.

Surface Area of Semi sphere = 360.20 m^2

The maximum stress a material can handle before permanent deformation is called the yield stress. The yield strength of the material is the maximum stress it can take before plastic deformation. For brittle-like materials like regolith, we take the yield and ultimate stresses to be the same.

From the properties of regolith discussed in earlier sections, we know that the maximum stress the structure can take is 34.5 MPa (tensile strength). Then the maximum force is,

Force = 34.5 MPa x 360.20 m^2 = 12.42 x 10^9 N.

5.6 Maximum size of Meteoroid on Structure

From Section 5.5, we can see that the maximum force our structure can sustain is 12.42 x 10^9 N. Now using this force we find the maximum size of the meteoroid that our structure can sustain before failure.

In a moving object like meteoroid, the dynamic energy can be expressed as $E = \frac{1}{2}mv^2$ and the work done at the time of impact can be expressed as $W = F * h$.

At the time of meteoroid impact, dynamic energy from the meteoroid is converted into work done on the structure. So, by combining both equations, we get

$$F = \frac{mv^2}{2*h} \qquad \text{Eq 5.1}$$

$$F = \frac{\rho * Vol * v^2}{2*h}$$

$$12.42 * 10^9 = \frac{1500 * 2\pi r^3 * 5500^2}{3 * 2h}$$

$$h = 3.825r^3$$

We take this *h* value in terms of *r* and substitute it into Eq 5.2,

$$3.825r^3 * (10^8)^{0.243} - 384.79\,[(1.5)(\tfrac{4\pi r^3}{3})(5.5)^2 - 0.013466(3000)(5.5)\left((1.5)\left(\tfrac{4\pi r^3}{3}\right)\right)^{\frac{5}{6}}(1.5)^{\left(-\frac{1}{3}\right)} -$$

$$0.3048\,(1.5)\left(\tfrac{4\pi r^3}{3}\right)(5.5)]^{\frac{1}{3}} > 0$$

$$87.902r^3 - 384.79\left[190.066r^3 - 897.791r^{\frac{5}{2}} - 10.533r^3\right]^{\frac{1}{3}} > 0$$

$$r > 250.07 \text{ mm.}$$

The maximum size of the meteoroid our structure can sustain has a radius of approximately 250mm. This number is, of course, very approximate.

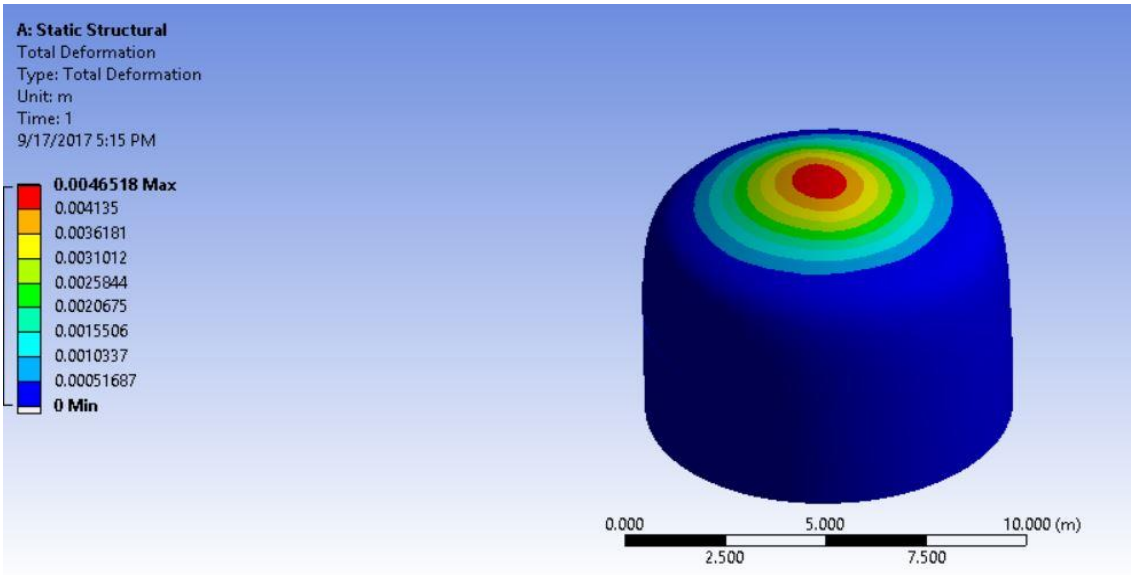

Figure 5. 1. Total deformation of the structure due to meteoroid impact

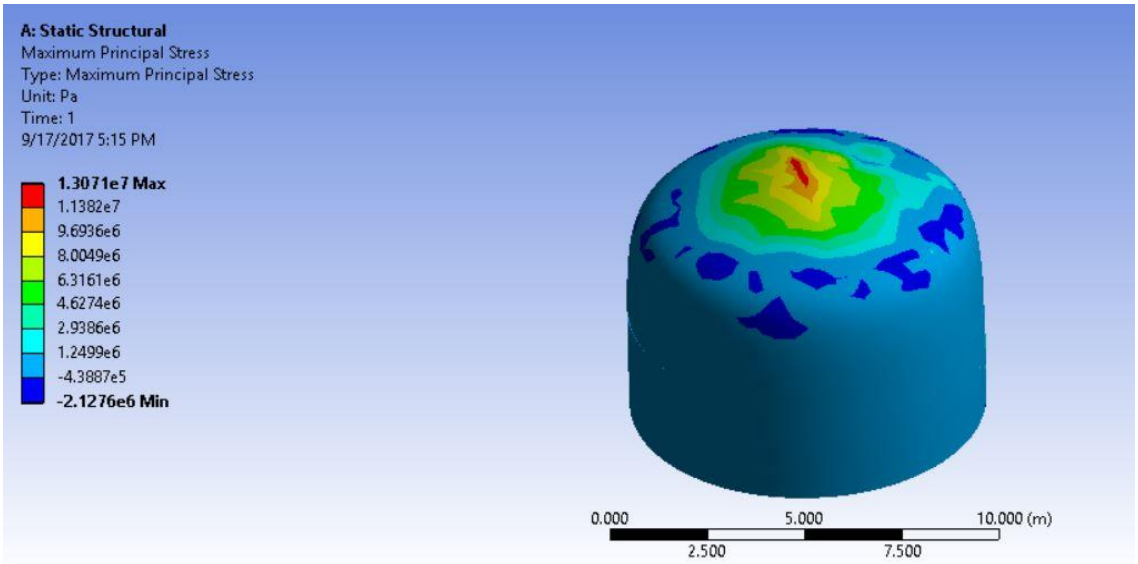

Figure 5. 2. Maximum principal stress on structure due to meteoroid impact

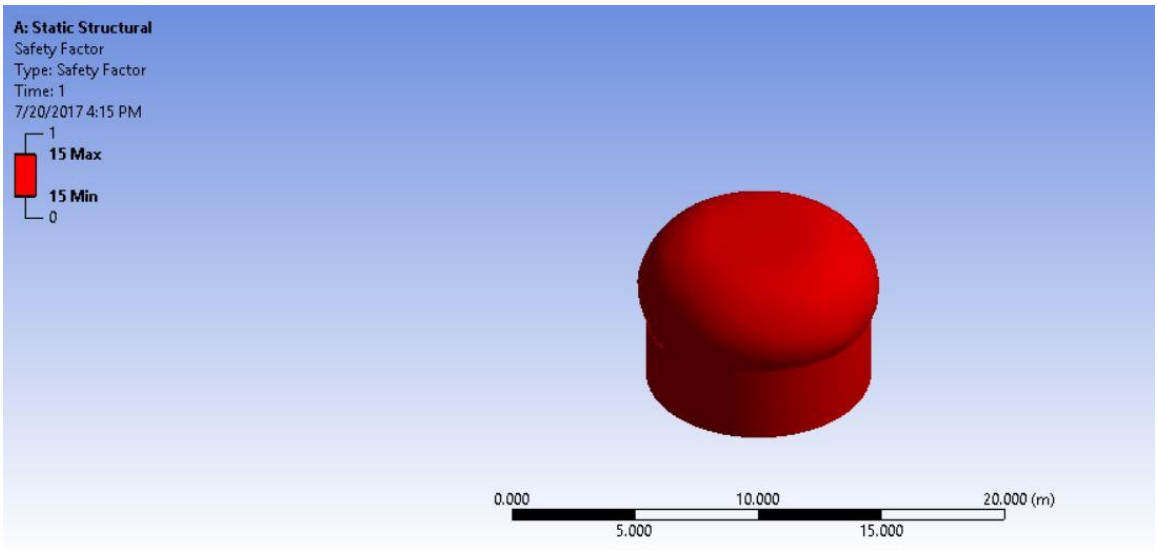

Figure 5. 3. Factor of safety

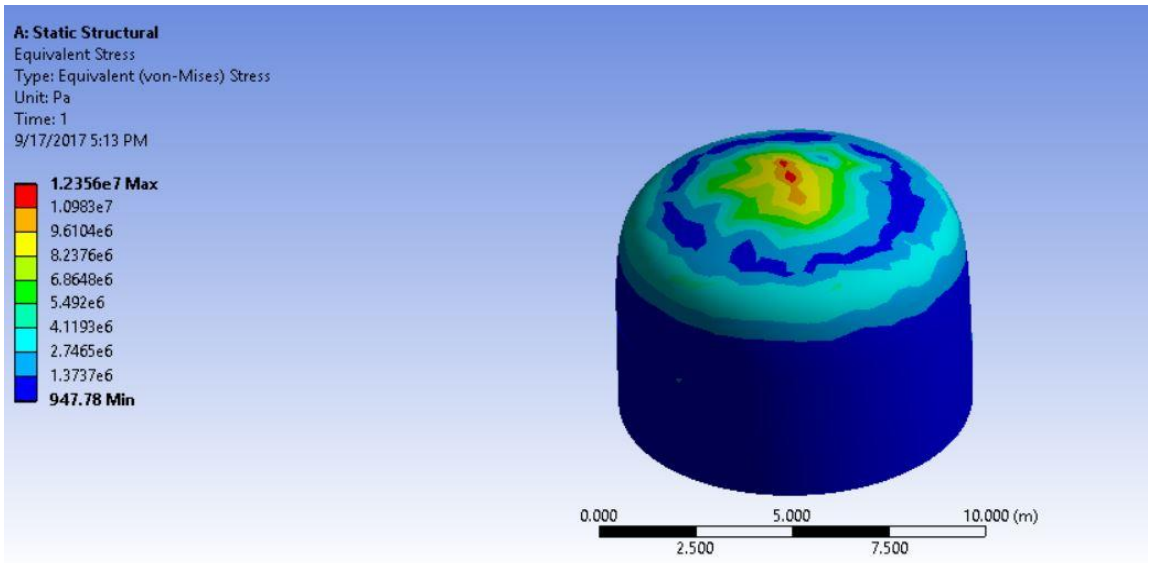

Figure 5. 4. Equivalent stress on structure due to meteoroid impact

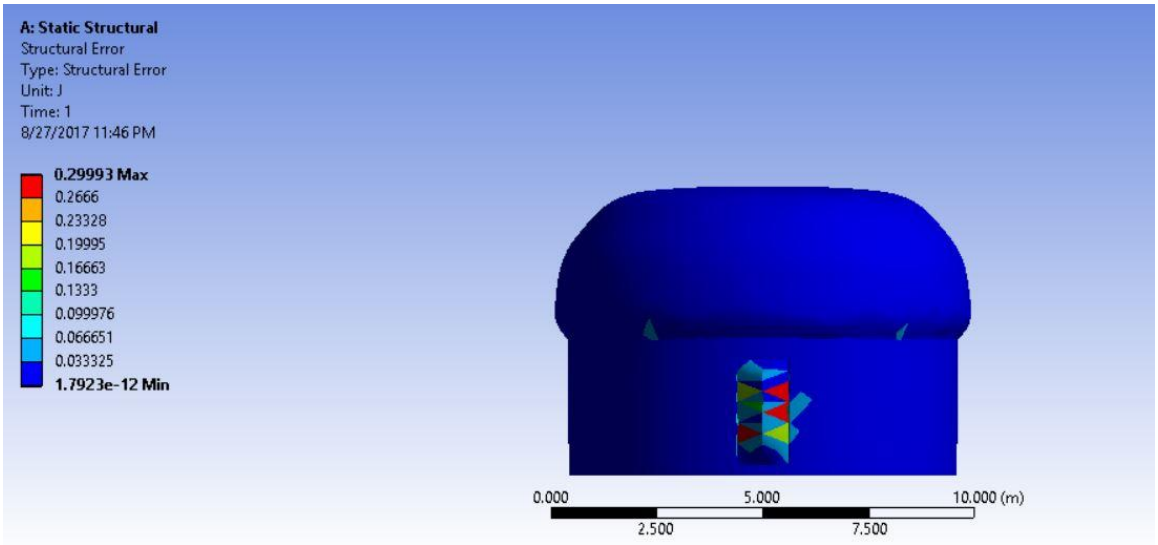

Figure 5. 5. Structural Error

5.7 Discussions and Conclusions

The two general forms of predicting failure criteria are the von Mises criteria and the maximum principal stress criteria. Both these criteria predict failure based on different mechanisms. Von Mises criteria uses distortion energy theory, and maximum principal stress criteria uses the maximum principal stress theory.

Maximum Principal Stress theory

This theory proposes that the failure will occur when the maximum principal stress in a structure is higher than the maximum strength at the elastic limit.

Distortion Energy Theory

In this theory, the total strain energy is divided into volumetric strain energy and shape strain energy. This theory proposes that failure occurs when the maximum value of distortion energy per unit volume in the material reaches the distortion energy per unit volume required to cause yield in a tensile test of same material.

The von Mises failure criterion is known for its approach based on strain energy. This criterion is mostly used for ductile materials. On the other hand, the Maximum Principal Stress theory has very limited applications, and is mostly used for brittle materials.

From the above Figures 5.1, 5.2, 5.3, 5.4 and 5.5, we can see that the maximum total deformation of the structure is 4.65 mm, which is almost negligible. Also, the maximum equivalent/von Mises stress acting on the structure is 12.35 MPa, which is well below the yield strength of the material. In addition to the von Mises stress, we have also simulated maximum principal stresses. From Figure 5.3, we can see that the maximum principal stress acting on the structure is 13.07 MPa, which is well under the breaking strength. Considering that the structure is to be built on the Moon, we generally consider high factors of safety since we have so many unknown parameters affecting the structure. We can see that the entire structure has high factor of safety, which is more than acceptable, and suggests that the structure is overdesigned, and can be scaled back, even with the many uncertainties we face.

All the above simulations and discussions from Figures 5.1 – 5.5 are for the meteoroid of radius 1mm, as the structure needs to sustain soil abrasion, lunar dust and smaller meteoroids. The meteoroid impacts generally range from meteoroids of radii of about 1mm to several mm. Any large meteoroid impact can be considered to lead to a structural failure, as it is almost impossible to design structures for such impact loads. From Section 5.6, we can see that the structure can sustain impact loads due to meteoroids of radii up to 250 mm, travelling at a maximum speed of 5.5 km/s. We note that such high impact resistance is due to the very high factor of safety that we have built into the structure. Of course, if this factor of safety is reduced, we expect a reduced capacity to meteoroid

resistance. Figure 5.5 shows some irregularities, asymmetries in the stresses, where we expect symmetry. Structural error is defined as the stress error energy divided by the total strain energy. In Figure 5.5, we can see that the maximum error is 29%, occurring at the doorway on the magnesium base. The entire structure, excluding the doorway, has a percentage stress error of less than 5%, which is acceptable for our purposes. Due to limitations in our meshing, we were not able to refine the mesh at the doorway, as we don't have the computational power for more elements. Although we have a factor of safety more than 15, ANSYS can only show a maximum factor of safety of 15 which is shown in the figure 5.3.

We can improve the results and lessen the approximations if we can run the simulations without any restrictions. Due to computational restraints, we have followed a very crude way of converting the dynamic impact of a meteoroid into a point load. We would get better understanding if we could solve the problem using dynamic simulations. Also, due to the restriction on the total number of elements, we could not refine the mesh, which causes the structural error. Although structural error is common, even when we refine mesh, it is desirable to see the estimated percent error reduced in future work.

Chapter 6. Future Work & Summary of Accomplishments

6.1 Performance-Based Engineering (PBE)

There are hundreds of papers on lunar structures, many offering unique approaches. Taking into account the many factors that need to be considered in designing a lunar structure, it a challenge to favor one design over the others. However, the majority of the research is devoted to innovative designs that, in principle, are able to overcome the challenges that the hostile lunar environment imposes. These detailed designs are mostly evaluated by considering the static analysis of the structures, while the other factors are just mentioned.

Performance-based engineering is a design approach that links the structural design to its end-user, where the outputs are the decision variables of use to the end-user. Generally, one can break this design framework into a sequence of four aspects:

1. Hazard Analysis
2. Structural Analysis
3. Damage Analysis
4. Loss Analysis

Performance-based engineering addresses system-level performance in terms of risk of significant event, fatalities, repair costs, and post-event loss of function. The design process is structured to meet specific performance expectations of the structure's occupants, owner and public.

Hazard Analysis Hazard analysis results in frequencies of occurrence of key events. For a lunar structure or facility, examples of key events include meteoroids, radiation, possible accidents, and structural aging/degradation.

Structural Analysis Analysis is performed in terms of system and component uncertainties. Thus, a lunar structural analysis includes structural member strength and geometric properties, regolith mechanics, internal pressurization, dynamic and impact loads, thermal and gradient loads, and other material aspects.

Damage Analysis Fragility curves are used to probabilistically model damage.

Loss Analysis Frequency and probability data can be used to extract performance metrics that are meaningful to facility stakeholders, metrics such as upper bound economic loss during the owner-investor's planning period.

Now risk-management decisions can be made based on the loss analysis. The figure below shows a generic equation formally depicting how the four steps of a performance-based engineering methodology lead to decision variables. One begins with an intensity or input that feeds into the structural response that feeds into fragility-based damage estimates that result in cost estimates in terms useful to the facility owner.

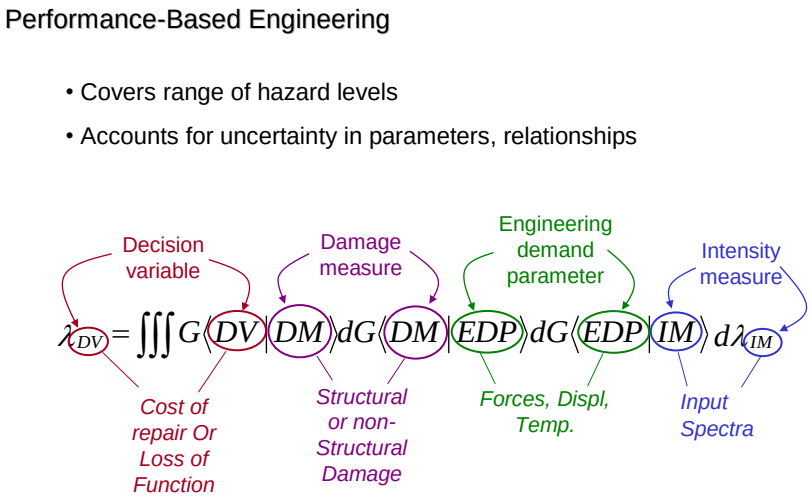

Figure 6. 1. Performance Based Engineering

Performance-Based Engineering (PBE) is a general approach that allows engineers to consider and assess the performance of complex mechanical systems subject to both natural and man-made hazards by taking into account the applicable uncertainties. With the PBE approach, the engineer can: (i) define clearly the performance aims for the structural system during its anticipated lifespan, (ii) meet the performance objectives by gaining advantage of specific criteria and validating them, and (iii) develop the structural design and exploit the innovative methodologies for an improvised design.

PBE was originally introduced for nuclear power plants, but in the last two decades, earthquake engineering has seen substantial research efforts in the development of PBE. Recently, this procedure has been extended to other situations such as tsunami and wind engineering. In all of the above applications, design of structural systems was

based on a realistic and reliable calculations of the threats associated with such hazards, which leads to a more effective use of resources.

By considering all the above advantages, we would like to apply performance based engineering framework procedures on inflatable space structures in our future studies.

A generic equation for Seismic Performance Assessment, for example, is,

$$\lambda\,(\mathrm{DV}) = \iint \mathrm{G}\left(\frac{\mathrm{DV}}{\mathrm{DM}}\right) \mathrm{dG}\left(\frac{\mathrm{DM}}{\mathrm{IM}}\right) \mathrm{d}\lambda\,(\mathrm{IM})$$

where DM are Damage Measures, IM are Intensity Measures, and DV are Decision Variables.

In all of the above applications, the designs of structural systems were based on a realistic and reliable calculations of the threat associated with such hazards, which lead to a more effective use of resources.

But this equation can't be replicated for lunar surface, as we have to deal with both range and magnitude, which are independent of each other for moonquakes. So, we need a double probability density function that depends on both magnitude and range, and independent of each other. One such function is the two-parameter Weibull density function,

$$\mathrm{F}_{\mathrm{Y\,|\,M,\,R}}(\mathrm{y}|\mathrm{m},\,\mathrm{r}) = \frac{m}{r^m}\,\mathrm{y}^{(\mathrm{m}-1)}\,e^{-(y/r)^m}$$

$$0 < \mathrm{y} < \infty$$

$$\mathrm{m} > 0$$

$$r > 0.$$

While we put some effort into applying PBE to the lunar structural problem, we were challenged by the lack of data, and also the numerical aspects of the integration domains, which are unclear. We believe that PBE is an excellent framework, but beyond the scope of this study.

6.2 Summary of Accomplishments

We have reviewed the literature on lunar habitats, especially inflatable concepts. We have developed a new concept for a hybrid-inflatable structural habitat for the lunar surface. We have considered the choice of materials for the inflatable part of the hybrid structure, as well as the foundation base for the structure. We have developed the concept for the connection between the solid and the Kevlar. This is a challenge when working with inflatable structures.

We have also worked with a simplified model for meteoroid impacts in order to obtain a very approximate estimate for the ability of the structure to resist a certain class of meteoroids.

References

[1] Anonymous 2017, "**India Eying Moon as Energy Source, ISRO Professor Tells Seminar**," **2017**(02/20) .

[2] Dr. Costa, C., and Dr. Mitch, T., 1995, "Inflatable Structures Technology Development Overview," Space Programs and Technologies Conference, Tustin, CA, pp. 2-3.

[3] Scherrer, I. J., 2012, "Geometric Control of Inflatable Surfaces," pp. 16-17-19.

[4] MOTTAGHI, S., 2013, "Design of a Lunar Surface Structure," pp. 20.

[5] Ruess. F, Schaenzlin. J, and Benaroya. H, 2006, "Structural Design of a Lunar Habit," pp. 135-136,137.

[6] Benaroya, H., Bernold, L., and Chua, K. M., 2002, "Engineering, Design and Construction of Lunar Bases," **15**(02) pp. 8-9.

[7] Dismukes, K., 2003, "TransHab Concept," **2003**(06/27) .

[8] Anonymous 2016, "Genesis I & II, Bigelow Aerospace's Pathfinder Spacecraft Program," **2006**(07/12) pp. 2.

[9] David, L., 2007, "Bigelow Aerospace's Sets a Business Trajectory," **2007**(03/26) pp. 1.

[10] Hinkle, J., Timmers, R., Dixit, A., 2009, "Structural Design, Analysis, and Testing of an Expandable Lunar Habitat." Anonymous American Institute of Aeronautics and Astronautics, NASA Langley Research Center, Hampton, VA, 23681, **50,** .

[11] Anonymous 2016, "BEAM: The Experimental Platform," **2016**(04/06) .

[12] Spudis, P., 2006, "Ice on the Moon," Thespacereview.Com, **2016**(07/16) .

[13] Bussey, D. B. J., Robinson, M. S., and Spudis, P. D., 2004, "IDEAL LANDING SITES NEAR THE LUNAR POLES," 35th Lunar and Planetary Science Conference, Anonymous League City, Texas, .

[14] Zimbelman, R. J., "The Apollo Landing Sites," .

[15] Zuber, T. M., Head, W. J., SMith, E. D., 2012, "**Constraints on the Volatile Distribution within Shackleton Crater at the Lunar South Pole.**," Nature, International Weekly Journal of Science, **486**(378-381) .

[16] Molloy, E., 2011, "Guide to the Stephanie Kwolek Innovative Lives Presentation." Smithsonian National Museum of American History, Kenneth E. Behring Center., pp. 2.

[17] Anonymous "Light in Weight, High in Performance - Kevlar Fiber." Http://Www.Dupont.Com/Products-and-Services/Fabrics-Fibers-Nonwovens/Fibers/Brands/Kevlar/Products/Dupont-Kevlar-Fiber.Html, .

[18] Anonymous "Kevlar Properties," Http://Www.Dupont.Com/Products-and-Services/Fabrics-Fibers-Nonwovens/Fibers/Articles/Kevlar-Properties.Html, .

[19] Landis, G. A., 2007, "Materials Refining on the Moon," Acta Astronautica, **60**(10-11) pp. 906-915.

[20] Taylor, L. A., and Carrier, W. D., 1993, "Oxygen Production on the Moon-an Overview and Evaluation," In: Resources of Near Earth Space. Lewis, J.S., Matthews, M.S., and Guerrieri, M.L., Eds., University of Arizona Press, Tucson, AZ, pp. 69-108.

[21] Watarai, H., 2006, "Trend of Research and Development for Magnesium Alloys," Science & Technology Trends - Quarterly Review, **18**pp. 84-97.

[22] Boby, A., Pillai, U. T. S., and Pai, B. C., 2011, "Developments in Magnesium Alloys for Transport applications—An Overview," Indian Foundry J., **57**(1) pp. 29-37.

[23] Jayalakshmi, S., Kailas, S. V., and Seshan, S., 2002, "Tensile Behaviour of s Ueeze Cast AM100 Magnesium Alloy and its Al2O3 Fibre Reinforced Composites." Composites Part A: Applied Science and Manufacturing, **33**(8) pp. 1135-1140.

[24] Cole, G. S., 2003, "Issues that Influence Magnesium's use in the Automotive Industry," Materials Science Forum, **419-422**pp. 43-50.

[25] Kaneko, T., and Suzuki, M., 2003, "Automotive Applications of Magnesium Alloys," Materials Science Forum, **419-422**(67-74) .

[26] Mordike, B. L., and Ebert, T., 2001, "Magnesium Properties, Applications, Potential." Materials Science and Engineering A, **302**(1-2) pp. 37-45.

[27] Liu, Y., and Taylor, L. A., 2011, "Characterization of Lunar Dust and a Synopsis of Available Lunar Simulants," Planetary and Space Science, **59**(14) pp. 1769-1783.

[28] Cortes, P., and Cantwell, W. J., 2004, "Fracture Properties of Fiber-Metal Laminates Based on Magnesium Alloy." Journal of Materials Science, **39**(3) pp. 1081-1083.

[29] Neelakanta, P. S., 1995, "Handbook of Electromagnetic Materials, Monolithic and Composite Versions and their Applications." CRC Press, .

[30] Shu, D. W., and Ahmad, I. R., 2011, "Magnesium Alloys: An Alternative for Aluminum in Structural Applications," Advanced Materials Research, **168-170**pp. 1631-1635.

[31] Wang, T., Debelak, K. A., and Roth, J. A., 2008, "Extraction of Magnesium and Copper using a Surfactant and Water in Supercritical Carbon Dioxide," Journal of Supercritical Fluids, **47**(1) pp. 25-30.

[32] Seboldt, W., Lingner, S., Hoernes, S., 1993, "Lunar Oxygen Extraction using Fluorine," In: Resources of Near Earth Space. Lewis, J.S., Matthews, M.S. , and Guerrieri, M.L., Eds., University of Arizona Press, Tucson, AZ, pp. 129-148.

[33] Benaroya, H., Mottaghi, S., and Porter, Z., 2012, "Magnesium as an ISRU-Derived Resource for Lunar Structures," **26**pp. 1-2-4.

[34] M, S., A, W., C, O., 2011, "Factors Impacting Habitable Volume Requirements," Center for Advanced Space Studies-Universities Space Research Association, pp. 2.

[35] Sharp, T., 2012, "What is the Temperature on Moon," SPACE.Com, **2012**(10/22) pp. 1.

[36] Happel, J. A., 2009, "Indigenous Materials for Lunar Construction," Applied Mechanics Reviews, **46**(6) pp. 313-325.

[37] William, R. J., and Jadwick, J. J., "Handbook of Lunar Materials," NASA Reference Publication 1057, .

[38] Steinberg, I. E., and Bulleit, W., 2003, "Reliability Analyses of Meteoroid Loading on Lunar Structures," **15**(1-2) pp. 53-54.